Appl Nanosci (2014) 4:185–188
DOI 10.1007/s13204-012-0187-4

ORIGINAL ARTICLE

Significance of $TiCl_4$ post-treatment on the performance of hydrothermally synthesized titania nanotubes-based dye-sensitized solar cells

Jeganathan Akilavasan · Kosala Wijeratne · Asangi Gannoruwa · A. R. M. Alamoud · Jayasundera Bandara

Received: 19 November 2012 / Accepted: 19 December 2012 / Published online: 13 January 2013

Abstract In this investigation, the effect of concentration of $TiCl_4$ for the post-treatment of hydrothermally synthesized titania nanotubes-based working electrode for dye-sensitized solar cells has been studied. Hydrothermally synthesized TiO_2 nanotubes were treated with different concentrations of $TiCl_4$ to investigate the effect of $TiCl_4$ concentration. The solar cell performance increased with the increase in $TiCl_4$ concentration up to 0.5 M and leveled off. The best solar cell showed a short-circuit current density (J_{sc}), open-circuit voltage (V_{oc}), fill factor (FF) and efficiency (η) of 12.75 mA/cm^2, 795 mV, 69.2 % and 7.04 %, respectively, while untreated TiO_2 nanotube showed J_{sc}, V_{oc}, FF and η of 2.4 mA/cm^2, 899 mV, 78.9 % and 1.7 %, respectively.

Keywords $TiCl_4$ treatment · Titania nanotubes · Dye-sensitized solar cells

Introduction

Dye-sensitized solar cells (DSSCs) have been identified as the best and promising alternative device for the conventional silicon-based devices with economically viable cost (Bisquert et al. 2004; Regan and Gratzel 1991). Highest efficiency of 11.2 % has been reported for mesoporous titania nanoparticles (TNPs)-based DSSCs (Chiba et al. 2006; Gao et al. 2008). However, due to high charge carrier recombination in TNP-based electrode, further enhancement of efficiency is a great challenge (Kim et al. 2006; Roy et al. 2011). To overcome the charge recombination problem in nanoparticles (NP), 1-D structures such as nanotubes (Lei et al. 2010; Park et al. 2008), nanorods (Liu and Aydil 2009; De Marco et al. 2010) and nanobelt (Dong et al. 2011; Pan et al. 2009) have been proposed and successfully implemented in DSSC. These 1-D structures are found to be promising substitute materials for the TNPs in DSSCs as they provide direct electron pathways and fast electron transport reducing charge carrier recombination (Enache et al. 2007; Lee et al. 2009). TNTs with different morphological structures have been successfully fabricated by anodization of Ti metal both on conducting glass and on Ti substrate (Chang et al. 2011; Yun et al. 2011). Despite superior beneficial factors such as fast electron transport and reduced charge recombination properties of 1-D TiO_2 structures, the reported efficiency for TNT-based DSSC is in the range of 6–7 % which is inferior to that of TNPs-based DSSC (Liao et al. 2011; Ye et al. 2011). Solar cell performance of DSSC has been improved significantly by post-treatment methods such as coating of an insulating layer on oxide–semiconductor (Wang et al. 2012) or by treatment of TiO_2-based electrode by $TiCl_4$ solution (Xin et al. 2011). Commonly applied post-treatment method involves immersion of TiO_2-based electrode in 0.04 M $TiCl_4$ solution followed by sintering at 500 °C. In this investigation, hydrothermally synthesized TiO_2 nanotube films were treated with different concentrations of $TiCl_4$ solutions for optimization of $TiCl_4$ post-treatment method for hydrothermally synthesized TiO_2 nanotube films. Solar cell performances of DSSC fabricated with hydrothermally synthesized TiO_2 nanotube films treated with different $TiCl_4$ concentrations were investigated and reported in this investigation.

J. Akilavasan · K. Wijeratne · A. Gannoruwa · J. Bandara (✉)
Institute of Fundamental Studies, Kandy, CP 20000, Sri Lanka
e-mail: jayasundera@yahoo.com

A. R. M. Alamoud
Department of Electrical Engineering, Sustainable Energy Technology (SET) Center, King Saud University (KSU), Riyadh, Kingdom of Saudi Arabia

Experimental

TNTs were synthesized via hydrothermal method (Kim et al. 2006). In hydrothermal method, 2 g of titania nanoparticles (P25 Degussa) were dispersed in 10 M $NaOH_{(aq)}$ solution by stirring for 30 min followed by transferring into a Teflon lined autoclave and kept at 150 °C for 48 h. The resultant product was washed with 0.1 M HCl and distilled water until the pH becomes 8.5. Once the pH of the TNT nanotube was reached 8.5, the nanotube paste was ultrasonicated for 10 min to make TNT suspension. Electrophoretic deposition (EPD) technique was employed to deposit TNT on the conducting substrate (FTO: F-doped SnO_2) using two electrode system with Pt wire as a counter while FTO as working electrodes. The electrolyte for EPD was prepared by mixing the TNT suspension and methanol in 2:1 (v/v) ratio and EPD was carried out at an optimized voltage of ~40 V for 6 min. The electrodeposited film was heated at 130 °C for 15 min and sintered at 450 °C for 30 min. For $TiCl_4$ treatment, 0.04, 0.1, 0.5 and 1.0 M concentrations of $TiCl_4$ (aq) were prepared from 99.9 % $TiCl_4$ (Sigma Aldrich). 30 µl of $TiCl_4$ of each concentration was placed on the pre-sintered TNT-coated FTO substrate for 30 min followed by removing excess $TiCl_4$ and finally sintered at 450 °C for 30 min. The $TiCl_4$-treated TNT films were immersed into 3 mM of N719 dye (Dyesol) solution for 3 h. Finally, the DSSC was assembled combining the working electrode and Pt counter electrode. Iodide/triiodide-based redox couple was utilized to complete the DSSC. The current–voltage measurements of test DSSCs were performed under one sun condition using a solar light simulator (New Port AAA solar simulator, AM 1.5 global, 100 mW/cm^2) with an active area of 0.25 cm^2. The intensity of the light was calibrated with a standard Si-reference cell. UV–vis absorbance spectra are measured by a Shimadzu 2450 UV–vis spectrophotometer. The external quantum efficiency (EQE) experiments were performed on Bentham PVE300 unit with a TMc 300 monochromator-based IPCE with a xenon arc lamp. A calibrated type DH Si photodetector was used as reference.

Results and discussion

Figure 1 shows the SEM image of the thin films of TiO_2 nanotube on FTO after annealing at 500 °C for 1 h. Randomly oriented TiO_2 nanotubes are clearly visible in The SEM image and the estimated size of the hydrothermally synthesised titania nanotubes are found to be ~250 nm in length and diameter of ~10 nm. The crystal structure of the product was also characterized by powder XRD method (figure not shown). The characteristic diffraction peak at 2θ of 25.3^o for titania anatase (101) crystal face is observed

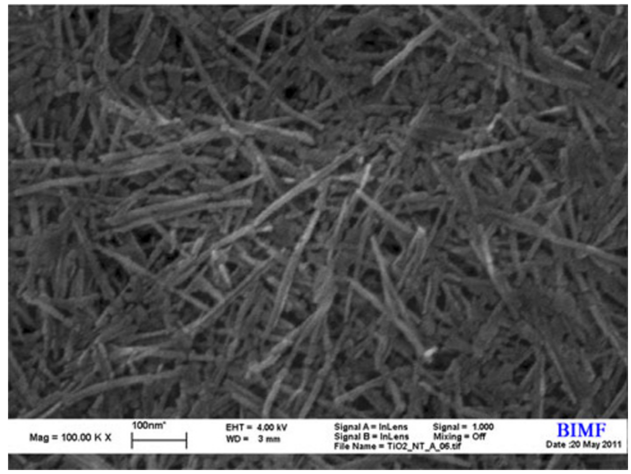

Fig. 1 SEM image of the hydrothermally synthesized TiO_2 nanotube films deposited on FTO glass by EPD method

and all the other peaks correspond to anatase TiO_2 that agree well with the standard reported values (JCPDS 21-1272) are also observed and absence of any other characteristic diffraction patterns indicating high purity of the prepared TiO_2 nanotube structures.

The current–voltage (*I–V*) characteristics of the DSSCs based on pristine and $TiCl_4$-treated TNT electrodes under the AM 1.5 G illumination at 100 mW/cm^2 are shown in Fig. 2 and the solar cell parameters are summarized in Table 1. Device fabricated with pristine TNT showed an V_{oc} of 899 mV, a short circuit current density (J_{sc}) of 2.4 mA/cm^2 and a FF of 78.9 %, resulting in a power conversion efficiency of 1.7 %. J_{sc} was increased to 8.1 mA/cm^2 after treatment of TNT films by 0.04 M $TiCl_4$

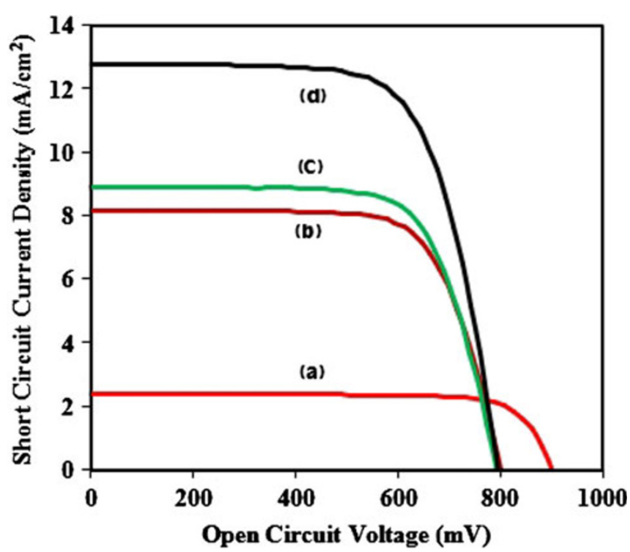

Fig. 2 *I–V* characteristics of **a** pristine TiO_2 nanotubes and **b** 0.04 M, **c** 0.10 M, **d** 0.50 M $TiCl_4$-treated TNT under the AM 1.5 illumination at 100 mW/cm^2 condition

Table 1 *I–V* characteristics of pristine TiO_2 nanotubes and $TiCl_4$-treated TNT under the AM 1.5 illumination at 100 mW/cm^2 condition

Electrode	J_{sc} (mA/cm^2)	V_{oc} (mV)	FF (%)	η (%)
Bare-TNT	2.4	899.2	78.94	1.70
0.04 M $TiCl_4$	8.15	801.1	71.55	4.68
0.10 M $TiCl_4$	8.85	791.5	71.12	4.98
0.50 M $TiCl_4$	12.75	795.4	69.25	7.04

solution and the J_{sc} increases with the increase of $TiCl_4$ concentration and a remarkable J_{sc} (12.7 mA/cm^2) was observed for the 0.5 M $TiCl_4$-treated TNT films. As shown in Fig. 2 and Table 1, a modest decrease in V_{oc} and FF is noticeable for the $TiCl_4$-treated TNT photoelectrode and also the decrease in both V_{oc} and FF with the increase in $TiCl_4$ concentration is noticeable.

The best solar cell showed a J_{sc}, V_{oc}, FF and η of 12.75 mA/cm^2, 795 mV, 69.2 % and 7.04 %, respectively, for the 0.5 M $TiCl_4$-treated TNT electrode. We have obtained even better solar cell performance for 1.0 M $TiCl_4$-treated TNT films than 0.5 M-treated films, but at such a high $TiCl_4$ concentration, we noticed the detachment of the electrodeposited TNT films from the FTO substrate and 0.5 M was taken as the best value. The significance of $TiCl_4$ post-treatment of hydrothermally synthesized TNT electrode is evident by more than fivefold enhancement in J_{sc} and four-fold enhancement in η compared to J_{sc} and η values of the pristine TNT films. Figure 3 shows the corresponding external quantum efficiency (EQE) results for the solar cell performance presented in Fig. 2 for DSSCs fabricated with TNT nanotube that are subjected to different $TiCl_4$ concentration. It can be seen from Fig. 3 that measured EQE spectra match the adsorbed dye spectra on TiO_2 (inset in Fig. 3), although the EQE at longer wavelengths is somewhat broader which may indicate a blue shift of the absorption spectrum of the adsorbed dye. The EQE measurements show that the $TiCl_4$ treatment affects the shape of EQE curves. Furthermore, the increase in the EQE spectral response in the 600–800 nm wavelength region with the increase of $TiCl_4$ concentration which could be attributed to the light scattering effect, that in turn enhances the light harvesting properties can be clearly noticeable.

As explained previously, the increase in J_{sc} and overall efficiency of DSSC fabricated with hydrothermally synthesized TNT nanotube with increasing $TiCl_4$ concentration compared to the solar cell fabricated with pristine TNT electrode is clearly noticeable. There could be several reasons for the observed $TiCl_4$ concentration effect on enhancing the solar cell performance. To investigate the reason for observed higher J_{sc} for TNT with increasing $TiCl_4$ concentration, we compared the dye adsorption

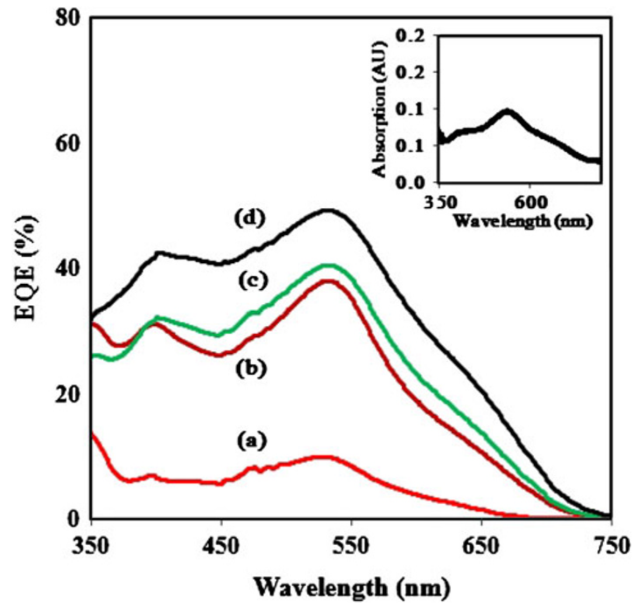

Fig. 3 External quantum efficiency of **a** pristine TiO_2 nanotubes and **b** 0.04 M, **c** 0.10 M, **d** 0.50 M $TiCl_4$-treated TNT under the AM 1.5 illumination at 100 mW/cm^2 condition

Table 2 Adsorbed dye amounts on pristine TiO_2 nanotubes and $TiCl_4$-treated TNT at different $TiCl_4$ treatment concentrations

Electrode	Dye loading (molecule/cm^2) × 10^{16}
Bare-TNT	2,048
0.04 M $TiCl_4$	2,409
0.10 M $TiCl_4$	2,770
0.50 M $TiCl_4$	3,492

amounts of both pristine TNT, $TiCl_4$-treated TNT with the variation of $TiCl_4$ concentration, and the results are given in Table 2. As given in Table 2, dye loading amounts increases after $TiCl_4$ treatment of TNT which could be due to formation of a thin film of titania particles around the TNT increasing surface roughness. Hence, observed increase in J_{sc} with the pre-treatment $TiCl_4$ concentration could be assigned to increase in dye loading amounts with the increase of $TiCl_4$ concentration. It has been reported that for both TiO_2 nanotube arrays fabricated by anodization and TiO_2 nanoparticle-based photoelectrodes, post-treatment with 0.04 M $TiCl_4$ resulted in enchancing the J_{sc} (Bandara et al. 2011; Sommeling et al. 2006). Compared to post-treatment method in the literature, in this investigation we used higher concentration of $TiCl_4$ solution. As shown in Tables 1 and 2, treatment of hydrothermally synthesized TiO_2 nanotube by 0.04 M $TiCl_4$ solution, enhances the dye loading and hence J_{sc} significantly. However, for hydrothermally synthesized TiO_2 nanotube photoelectrode, further increase in concentration of $TICl_4$ solution to 0.5 M resulted in enhance in J_{sc} which could be due to availability of more void space in electrodeposited TiO_2 nanotube photoelectrode compared to ordered arrays of TiO_2 nanotube photoelectrode. Even though the system described in this report needed much higher $TiCl_4$ concentration, it will not adversely affect the cost as the nanotube fabrication is much simpler and economical than the arrayed TiO_2 nanotube. We further investigated the series (R_s) and shunt (R_{sh}) resistances of TiCl4-treated TNT and bare TNT which can be obtained from the slopes of the *I–V* curves. With the increase in the concentration of pre-treatment $TiCl_4$ solution, decrease in the calculated R_s $(dV/dI)_{I=0}$ for TNT is noticeable while R_{sh} remains the same. Reduced R_s yielding faster charge transport and an optimum device operation and hence enhanced device performance for 0.5 M $TiCl_4$-treated TNT-based devices can be justified based on R_s values as well.

Conclusions

The investigation showed that the efficiency of the DSSC based on hydrothermally synthesized TNT can be improved significantly by the $TiCl_4$ treatment and the best solar cell was fabricated with 0.5 M $TiCl_4$-treated TNT electrode. Enhanced in dye loading and electron transport with the increase in $TiCl_4$ treatment was found to be the main reasons for enhanced solar cell performance.

Acknowledgments A NRC research grant (NRC 07-46) to purchase IPCE unit is highly appreciated. JB acknowledges the support from "Visiting Professor" program and Sustainable Energy Technology, Department of Electrical Engineering of King Saud University, Riyadh, KSA.

References

Bandara J, Shankar K, Basham J, Wietasch H, Paulose M, Varghese OK, Grimes CA, Thelakkat M (2011) Integration of TiO_2 nanotube arrays into solid-state dye-sensitized solar cells. Eur Phys J Appl Phys 53:20601

Bisquert J, Cahen D, Hodes G, Ruhle S, Zaban A (2004) Physical chemical principles of photovoltaic conversion with nanoparticulate, mesoporous dye-sensitized solar cells. J Phys Chem B 108:8106–8118

Chang YH, Lin HW, Chen C (2011) Ultrafast initial growth rate of self-assembled TiO_2 nanorod arrays fabricated by Ti anodization. Electrochem Sol Sta Lett 14:K1–K4

Chiba Y, Islam A, Watanabe Y, Komiya R, Koide N, Han L (2006) Dye-sensitized solar cells with conversion efficiency of 11.1 %. Jpn J Appl Phys 45:L638–L640

De Marco L, Manca M, Giannuzzi R, Malara F, Melcarne G, Ciccarella G, Zama I, Cingolani R, Gigli G (2010) Novel preparation method of TiO_2-nanorod-based photoelectrodes for dye-sensitized solar cells with improved light-harvesting efficiency. J Phys Chem C 114:4228–4236

Dong Y, Pan K, Tian G, Zhou W, Pan Q, Xie T, Wang D, Fu H (2011) Dye-sensitized solar cells based on TiO_2-B nanobelt/TiO_2 nanoparticle sandwich-type photoelectrodes with controllable nanobelt length. Dalton Trans 40:3808–3814

Enache PE, Boercker JE, Aydil ES (2007) Electron transport and recombination in polycrystalline TiO_2 nanowire dyesensitized solar cells. Appl Phys Lett 91:123116–123119

Gao F, Wang Y, Shi D, Zhang J, Wang M, Jing X, Humphry-Baker R, Wang P, Zakeeruddin SM, Grätzel M (2008) Enhance the optical absorptivity of nanocrystalline TiO_2 film with high molar extinction coefficient ruthenium sensitizers for high performance dye-sensitized solar cells. J Am Chem Soc 130:10720–10728

Kim GS, Seo HK, Godble VP, Kim YS, Yang OB, Shin HS (2006) Electrophoretic deposition of titanate nanotubes from commercial titania nanoparticles: application to dye-sensitized solar cells. Electrochem Commun 8:961–967

Lee BH, Song MY, Jang SY, Jo SM, Kwak SY, Kim DY (2009) Charge transport characteristics of high efficiency dye-sensitized solar cells based on electrospun TiO_2 nanorod photoelectrodes. J Phys Chem C 113:21453–21457

Lei BX, Liao JY, Zhang R, Wang J, Su CY, Kuang DB (2010) Ordered crystalline TiO_2 nanotube arrays on transparent FTO glass for efficient dye-sensitized solar cells. J Phys Chem C 114: 15228–15233

Liao JY, Lei BX, Wang YF, Liu JM, Su CY, Kuang DB (2011) Hydrothermal fabrication of quasi-one-dimensional single-crystalline anatase TiO_2 nanostructures on FTO glass and their applications in dye-sensitized solar cells. Chem Eur J 17: 1352–1357

Liu B, Aydil ES (2009) Growth of oriented single-crystalline rutile TiO_2 nanorods on transparent conducting substrates for dye-sensitized solar cells. J Am Chem Soc 131:3985–3990

Pan K, Dong Y, Tian C, Zhou W, Tian G, Zhao B, Fu H (2009) TiO_2-B narrow nanobelt/TiO_2 nanoparticle composite photoelectrode for dye-sensitized solar cells. Electrochim Acta 54:7350–7356

Park JH, Lee TW, Kang MG (2008) Growth, detachment and transfer of highly-ordered TiO_2 nanotube arrays: use in dye-sensitized solar cells. Chem Commun 25:2867–2869

Regan BO, Gratzel M (1991) A low-cost, high-efficiency solar cell based on dye-sensitized colloidal TiO_2 films. Nature 353: 737–740

Roy P, Berger R, Schmuki S (2011) TiO_2 nanotubes: synthesis and applications. Angewandte Chemie International 50:2904–2940

Sommeling PM, O'Regan BC, Haswell RR, Smit HJP, Bakker NJ, Smits JJT, Kroon JM, van Roosmalen JAM (2006) Influence of a $TiCl_4$ post-treatment on nanocrystalline TiO_2 films in dye-sensitized solar cells. J Phys Chem B 110:19191–19197

Wang S, Zhang X, Zhou G, Wang ZS (2012) Double-layer coating of $SrCO_3$/TiO_2 on nanoporous TiO_2 for efficient dye-sensitized solar cells. Phys Chem Chem Phys 14:816–822

Xin X, Scheiner M, Ye M, Lin Z (2011) Surface-treated TiO_2 nanoparticles for dye-sensitized solar cells with remarkably enhanced performance. Langmuir 27:14594–14598

Ye M, Xin X, Lin C, Lin Z (2011) High efficiency dye-sensitized solar cells based on hierarchically structured nanotubes. Nano Lett 11:3214–3220

Yun HG, Park JH, Baec BS, Kang MG (2011) Dye-sensitized solar cells with TiO_2 nano-particles on TiO_2 nano-tube-grown Ti substrates. J Mater Chem 21:3558–3561